![ALTA 2020 ONLINE NOVEMBER — 25 YEARS logo]

25th annual conference proceedings

Uranium-REE Conference

Including

Application of Membranes Forum

Sponsored by

16th annual uranium event

8th annual rare earth elements event

ALTA Metallurgical Services, Melbourne, Australia

www.altamet.com.au

Conference Proceedings

ALTA 2020 Uranium-REE Conference

Including

Application of Membranes Forum

18 November 2020, Online

ALTA Metallurgical Services Publications

All Rights Reserved

To purchase a copy of this or other publications visit www.altamet.com.au

celebrating 35 years of service to the global mining and metallurgical industry

ALTA Metallurgical Services (**ALTA**) was established in 1985 by Metallurgical Consultant and Managing Director, **Alan Taylor**, to serve the worldwide mining, minerals and metallurgical industries. ALTA offers a wide range of services and resources to the metallurgical industry.

High-level metallurgical and project development consulting.

Practically oriented live and online short courses presented by Alan Taylor. Topics include treatment of nickel laterites, copper ore leaching, uranium ore processing, copper SX-EW, heap leaching and solvent extraction.

ALTA conferences are a world-class annual metallurgical conference and a leading platform for innovation. It comprises five international conferences, panel discussions, short courses, and trade exhibition. It features highly focused programs, topical forums and presentations from key international speakers.

Technical proceedings and manuals from ALTA conferences and short courses for online purchase

MetBytes, free technical articles offering metallurgical commentary and insights.

Free resources, including proceedings from ALTA 1995-2019 Nickel-Cobalt-Copper, Uranium-REE, In-Situ Recovery, Gold-PM and Lithium & Battery Technology conferences for free download (1650+ papers). The ALTA free library is expanded regularly, providing a valuable ongoing resource to the industry.

RARE EARTH CONCENTRATE PROCESSING AND PURIFICATION. COMPARISON AND OPTIMIZATION USING OLI SIMULATION

By

[1]Louis de Klerk, [2]Gaurav Das and [2]Anthony Gerbino

[1]Northern Minerals, Australia
[2]OLI Systems, USA

Presenter and Corresponding Author

Anthony Gerbino
aj.gerbino@olisystems.com

ABSTRACT

We present a flowsheet simulation study of a three-step rare earth element (REE) hydrometallurgy processing plant. The steps consist of a sulphation kiln with water leach, counter-current-decantation (CCD), and a purification circuit. Our overarching goal was to optimize this part of the plant operations using rigorous thermodynamic modeling.

From a plant perspective, the following conclusions were made: 1) the current cooling of the kiln off gas recovers the bulk of the acid gases; 2) we were able to developed a relationship between off-gas temperature and amounts of HCl and H_2SO_4 exiting the first stage of scrubbing of the vent. This will allow better control of the scrubbing system to avoid gaseous emissions; 3) the current ratio of wash water:sludge feed entering the CCD circuit, recovers 99.9% of the dissolved REE from the leach residue, provided that fresh water used in the wash; and 4) some of the lime added in pH control may be underused because of slow precipitation, and the lime may continue to react in downstream purification steps where $Mg(OH)_2$ is used to reach the pH point of the second stage neutralizer.

We were able to achieve a mass balance of the plant operations using flowsheet simulation including chemical additive requirements and product / waste output. We also computed that Y, Gd, and Nd phosphates should precipitate in the CCD, even though they are not observed in plant operations. This is probably due to the slow precipitation kinetics associated with these phosphates. This may indicate that prolonged residence times of the pregnant leach may result in product loss.

Keywords: Rare earth, Processing, thermodynamics

INTRODUCTION/BACKGROUND

Plant Operations

Northern Minerals has constructed and is operating a pilot scale project aimed at assessing the technical and economic feasibility of a full-scale commercial operation at its Browns Range mine site adjacent to the Wolverine and Gambit deposits in Western Australia.

Figure 1 - Northern Minerals' Browns Range pilot plant

The test work program has commenced and first pilot plant production of rare earth carbonate was achieved in the December quarter of 2018 to test the pilot plant operation and to collect data to feed back into the processing flowsheet.

The pilot plant contains all the processing steps planned for a commercial plant. However, the plant is downsized to a capacity to process 60,000tpa of ore at 1.19% total rare earth oxides (TREO) through the beneficiation plant, and 3,200tpa of xenotime concentrate at 20% TREO through the hydrometallurgical process. The final product will contain 49,000kg dysprosium in 590,000kg TREO within a mixed RE carbonate per annum.

The hydromet circuit consists of a sulphation kiln, water leach, purification circuits and rare earth carbonate precipitation. The final product is a mixed rare earth carbonate, consisting predominantly of Yttrium and heavy rare earths. The ore concentrate also includes the following non-RE elements.

Table 1 - list of metals, anions, and oxyanions that comprise the ore concentrate used in this study

Group I and II	Transition metals (first row)	Other	Actinides	Anions and oxyanions
Na(I)	Cr(III)	Zr(IV)	U(VI)	AsO_4^{-3}
K(I)	Mn(II)	Sn(IV)	Th(IV)	Cl^{-1}
Mg(II)	Fe(III)	Al(III)		PO_4^{-3}
Ca(II)	Co(II)	Inerts		SO_4^{-2}
Sr(II)	Ni(II)			SbO_4^{-3}
Ba(II)	Cu(II)			SiO_2
	Zn(II)			

Thermodynamic Research

The first-principle's research group at OLI developed a thermodynamic database for modeling REE reactivity. The project was funded in part by the US Department of Energy (DOE), with the purpose of developing domestic sources of rare earth elements. The initial systems studied were the rare earth oxides,

oxyhydroxides, and hydroxides[2]. More recent, unpublished systems include sulfates, halides, and selected phosphates, carbonates, and molybdates. The table below contains the status of the current research.

Table 2 - Current state of the thermodynamic database development for rare-earth elements
(Green complete , Red outstanding)

	O, OOH, (OH)	SO$_4$	Cl	Br	I	F	PO$_4$	S	CO$_3$	Org Acid	NO$_3$	MoO$_4$	Total phase
La	G	G	G	G	G	G	R	G	R	R	G	G	10
Ce	G	G	G	G	G	G	R	G	R	R	G	R	11
Pr	G	G	G	G	G	G	R	R	R	R	R	G	10
Nd	G	G	G	G	G	G	G	G	G	G	R	G	12
Sm	G	G	G	G	G	G	R	R	R	R	R	G	8
Eu	G	G	G	G	G	G	G	R	R	G	G	R	7
Gd	G	G	G	G	G	G	G	R	R	G	R	G	27
Tb	G	G	G	G	G	G	G	R	R	G	G	R	11
Dy	G	G	G	G	G	G	R	R	R	R	R	G	8
Ho	G	G	G	G	G	G	R	R	R	R	R	G	5
Er	G	G	G	G	G	G	R	R	R	R	R	R	8
Tm	G	R	G	G	G	G	R	R	R	R	R	R	6
Yb	G	G	G	G	G	G	R	R	R	R	R	G	8
Lu	G	G	G	G	G	G	R	R	R	R	R	G	8
Yb	G	G	G	R	G	G	G	R	R	G	G	G	8

The Combined Plant-Database Effort

The ore concentrate contains fifteen rare earth elements and thirty accessory elements. This creates a chemical system containing ~290 aqueous species, 11 vapor species, and ~460 potential solid phases (147 of these solids contain REE). Thus, the plant process being studied provided an opportunity to test the accuracy of the new database and to see how this research can be used to optimize plant operations.

PLANT OPERATIONS

The plant operations that have been modelled are presented into three separate processes:

Sulphation Kiln Process

The sulphation kiln is fed with a rare earth phosphate concentrate (Mainly xenotime or YPO$_4$) and 98% sulphuric acid, and produces an apparently dry solid containing sulphuric acid at the kiln outlet conditions and a gaseous stream consisting of air and a range of sulphurous gases.

Figure 2 - Indirectly heated rotary kiln

Water Leach and Counter-Current Decantion (CCD) Process

The kiln product is fed to a water leach circuit to take the rare earth elements into solution. The CCD circuit uses six CCDs in series to wash solids and recover soluble components before the leach residue solids are discarded. The washed solids are mostly silica and iron phosphates with other sulfates, phosphates, and oxides/hydroxides.

Figure 3 - CCD Circuit

Purification Process

The purification circuit produces a purified, mixed REE solution. The circuit aim is to minimise REE losses with the solid waste at the intermediate pH steps. There are several stages in the purification circuit including ferric addition, lime addition and a two-stage magnesia addition. The lime and magnesia stages are controlled to particular pH levels. The purified liquor produces rare earth carbonates at the back end of the process.

Figure 4 - Purification Circuit

SIMULATION APPROACH

Each of the three plant processes were modeled separately to simplify the work and the interpretation. Also, since the chemistry across the three processes vary significantly, separating the processes reduced the chemistry range that needed to be computed, which reduces calculation runtime and report length.

Sulphation Kiln Simulation

The sulphation kiln unit is depicted below (Figure 5). The *98% H2SO4* and *Dried Concentrate* enter a mixer unit. The mixed slurry (*595 Bake Oven Feed*) and *Air* is fed to a kiln operating at 275 C and ambient pressure. A *Dummy water-in* stream containing pure H_2O also enters the kiln and is used to help the reactor converge (a simulation technique). Immediately downstream of the kiln, a component splitter removes that same amount of H_2O added (*Dummy water Out*).
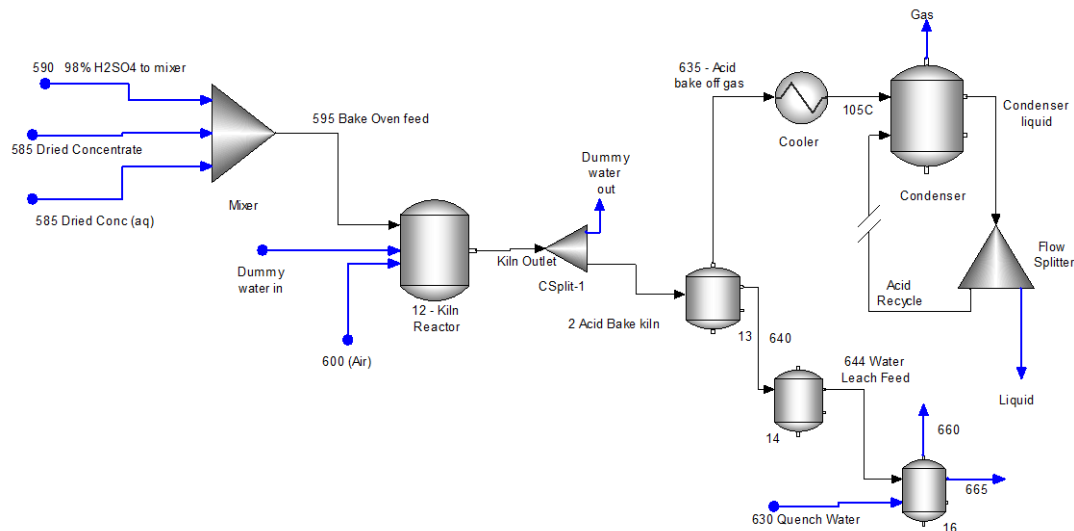

Figure 5 - Simulation of the Sulphation kiln. The dummy water in and dummy water out streams were added to enable the 12-Kiln Reactor to converge. All other processes were modeled as reported.

The kiln input is shown in Table 3 below. It is about 54% H_2SO_4 and 46% Xenotime ore concentrate. Approximately forty elements enter the kiln.

Table 3 - Chemical components of the kiln feed, including the 98% H_2SO_4 and ore concentrate

Key inflows	Rare Earth Element		Major Gangue Element	Minor Gangue Element	
H_2SO_4	Y	Tb	Fe	Co	Sr
SiO_2	La	Dy	Al	Mn	Ba
PO_4^{-3}	Ce	Ho	Ca	Cr	Na
H_2O	Pr	Er	K	Ti	Zr
	Nd	Tm	Mg	Ni	As
	Sm	Yb	Inert	U	Sb
	Eu	Lu		Th	Zn
	Gd			Cl	Pb
				Cu	Sn

The product from the Kiln reactor is separated into vapor (*635-Acid bake off gas*) and solid (*640*). The *635-Acid bake* off *gas* is cooled and the *Gas* (mostly air components) is separated from the *Condensed Liquid*. A portion of the condensed liquid is recycled back to the Condenser, and the *Liquid* exits the process for H_2SO_4 recovery and / or disposal. The target cooling temperature is based on removing sufficient $H_2SO_4/SO_3/HCl$ from the gas so that it is not corrosive at its dew point.

The rich REE solid (640) is sent to a water leach tank (Unit 16) where is contacted with Quench/Leach water. This leached REE slurry (Stream 665), is then fed to the CCD process.

Counter Current Decantation Simulation

The counter-current decantation configuration is shown below (Figure 6). The *leached REE slurry* (stream 665) enters CCD-1 and follows the path (right to left):

665--›770--›780--›790--›820--›830--›840.

The *wash water* (stream 885) enters CCD-6 and follows the path:

855--›845--›835--›825--›795--›785--›775.

The inlet streams (815, 810, 805, 765, 760, and 755) contains low flow rates of additional wash water originating from flocculant addition.
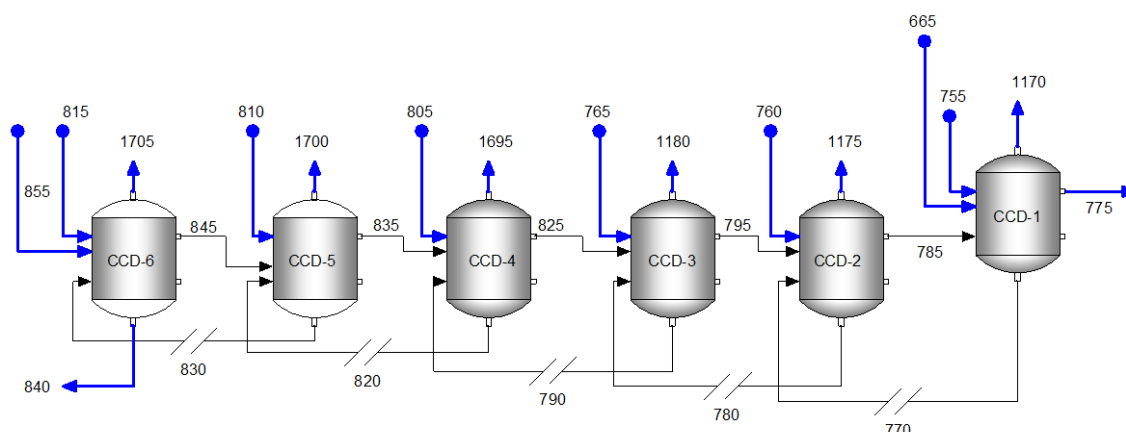

Figure 6 - Simulation of the Counter Current Decanter. The unit contains six washing stages.

Stream 775 is the *rich REE leachate liquor* that is sent to the purification unit. It is an acidic sulfate and phosphate solution. Stream 840 contains the washed solids that are sent to disposal. Each mixing tank is adiabatic (temperature not controlled) and complete mixing before separation within the tank is assumed.

Purification Simulation

The purification configuration is shown below (Figure 7). The rich REE leachate liquor (Stream 775) enters the purification circuit (left of image) and undergoes a series of pH neutralization steps where impurity solids are precipitated at each stage. The purified REE solution then is then neutralised with sodium carbonate to produce a RE-carbonate solids (Stream 1150).
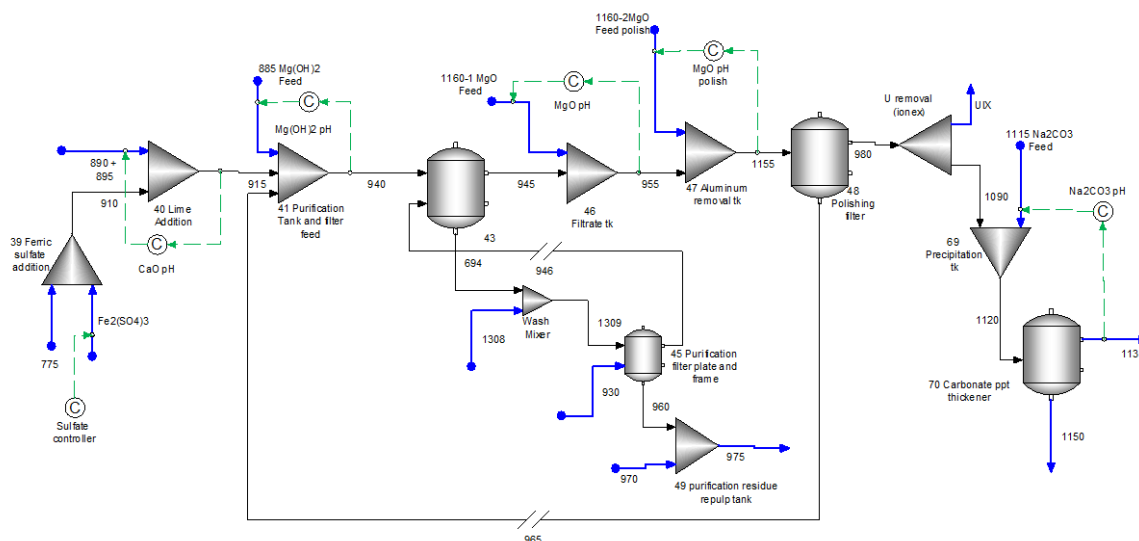

Figure 7 - Simulation of the Purification process. Several of the process units (mixers, valves, etc.) are removed in this image to simplify interpretation.

There are six chemical reaction steps:

1. Add $Fe_2(SO_4)_3$ and precipitate excess PO_4^{-3} from the solution.

2. Add CaO to raise the pH and precipitate excess SO_4^{-2} from solution (as $CaSO_4$).

3. Add $Mg(OH)_2$ to raise the pH and to precipitate non-REE metal hydroxides

4. Add $Mg(OH)_2$ to further raise the pH and to precipitate all remaining Al and some REE

5. Remove uranium from the filtered liquor using an ion-selective resin.

6. Add Na_2CO_3 to remaining liquor and precipitate the rare earth carbonates.

This process includes two sludge recycle circuits. The inner circuit removes $Al(OH)_3$, $Fe_2(SO_4)_3$, and $CaSO_4$ from the process stream. These solids are washed (wash mixer) and the filtrate is returned to the process. The outer recycle loop recycles an $Al(OH)_3$-rich sludge which is used to remove Al and recover rare earths and in part aids in precipitation and recovers excess alkalinity.

There are six flow controllers. The first controls the stoichiometric amount of Fe^{+3} needed to remove phosphate. The remaining controllers fix the stream pHs at target pHs by a CaO controller, a $Mg(OH)_2$ controller, a MgO controller , a MgO controller, and a Na_2CO_3 controller.

All calculations are set to adiabatic and ambient pressure. Reactions are assumed to be complete at each step (no rate-limiting reactions assumed).

RESULTS – SIMULATION AND PLANT OPERATIONS

Sulphation Kiln Process

Process Operations

The kiln used is an indirectly fired rotary kiln that heats the acid / concentrate mixture to the reaction temperature and maintains it at temperature for a prescribed residence time. The use of an indirectly heated kiln allows for a much lower volume of contaminated off gases compared to a directly fired kiln but at the expense of being more vulnerable to scale formation. Off gases are cooled by flash cooling in a venturi scrubber before being scrubbed in a series of towers before being released to atmosphere.

The purpose of simulating the kiln was to understand the chemical outputs of the acid-bake discharge (Stream 2), the cooler gas (gas), the water leach feed (Stream 644), and the quench / water stream (stream 665). The acid-bake kiln discharge was computed to contain solids, liquid, and vapor at 275°C (Table 4).

Table 4 - Mass balance around the kiln discharge

Kiln outlet	Simulated
T, °C	275
Mass rate, kg/hr	100%
Liquid rate, kg/hr	43%
Solid rate, kg/hr	26%
Vapor rate, kg/hr	31%

The liquid is a mixture containing 58% H_2SO_4, 20% H_3PO_4, 5% $MgSO_4$ plus other dissolved metals. The H_2O content is less than 0.5% (non-aqueous electrolyte liquid). The solid stream is a combination of non-RE metal sulfates (Ba, Ca, Cr, Ni, Pb, and Zn), REE-sulfates ($La_2(SO_4)_3.8H_2O$, $Na_2La_2(SO_4)_4.2H_2O$, and $Y_2(SO_4)_3$), Sb_2O_5, SiO_2, and inerts. By comparison plant operations report a single acid-containing solid phase at the exit temperature of about 150° C.

Since the liquids and solids are not separated prior to water leaching, the uncertainty in the actual liquid-solid ratio can be ignored for this report. Stream 644 is then quenched with water leach water. The mixture cools to about 71° C and the ionic strength reduces to about 1.5 molal, about three times the salinity of seawater. Such conditions are well within the framework of the activity model used in these predictions.

Table 5 - the Kiln solids remaining after quenching to 71°C.

Rich liquor	Simulated
T, °C	71
Solid Mass rate	23% of solids feed
ash	0.4%
$BaSO_4$	0.03%
$EuPO_4$	0.06%
SiO_2	55%
TiO_2	0.2%
YPO_4	44%
ZrO_2	0.006%
SrSO4	0.016%

The water leach feed (Stream 644) contains dissolved rare earth elements, metals, phosphates, and sulfates. It also contains undissolved silicates, sulfates, oxides, and inerts. The ionic strength is computed to be 0.894 mol/mol (mole-fraction basis). Such systems are ionic liquids, and an activity model is required to compute the volatility of gases and reactivity of cations and anions[3].

YPO_4 and $EuPO_4$ are computed to precipitate. Yet this is not observed in the plant, and the process would not be viable if these REE phosphates were precipitated. This problem also persists in the CCD and Purification units, and so both phases plus $GdPO_4$, $TbPO_4$, and $NdPO_4$ are removed from all calculations. It should be noted that the thermochemical data from literature sources used to study $REEPO_4$ correspond to crystalline anhydrous minerals, which could form very slowly, somewhere between 5-100 days depending on the nature of the rare earth element[4,6,5] . At present, it is not possible to predict the transient solubility of an intermediate (possibly amorphous) phosphate phase that forms over the time scale of the process.

The acid-bake-off gas, which is mostly air resulting from leaks into the kiln system, is computed to contain 12% H_2O, 13% H_2SO_4, 4% SO_3, and trace amounts of HCl. The plant off gases are scrubbed before release to remove and remaining contaminants.

Table 6 - Composition of Acid bake off gas

	Off gas
	Simulated
H_2O	6.5% by mass
N_2+O_2	93% by mass
HCl	0.00001% by mass
H_2SO_4	0.00001% by mass

When this gas is condensed to 105°C, the H_2SO_4 and HCl concentrations in the vapor reduces to ~200 ppbV. Figure 8 is the acid content in the separated gas as the condenser temperature varies from 110 to 90°C. HCl is computed to be largely independent of cooler temperature. H_2SO_4 however is computed to vary by a factor of 20 over the same temperature range.
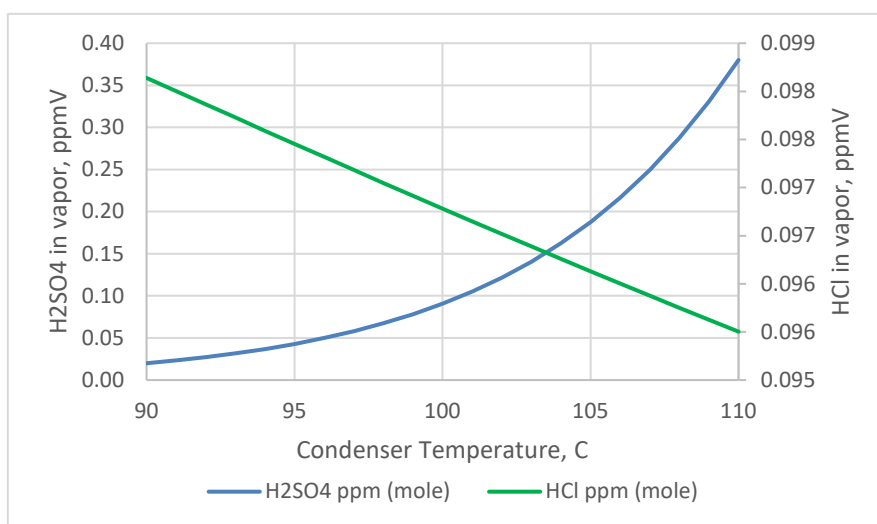

Figure 8 - H_2SO_4 and HCl in separated gas after cooling. The lower the cooling temperature the lower the H_2SO_4 fraction on the separated gas. HCl is less sensitive to condenser temperature.

Figure 9 is the calculated temperature at which this separated gas condenses if cooled downstream of the condenser. The gas dew point temperature and the dew point pH are both dependent on the condenser temperature. This is because the H_2SO_4 fraction in the gas phase varies with condenser temperature.
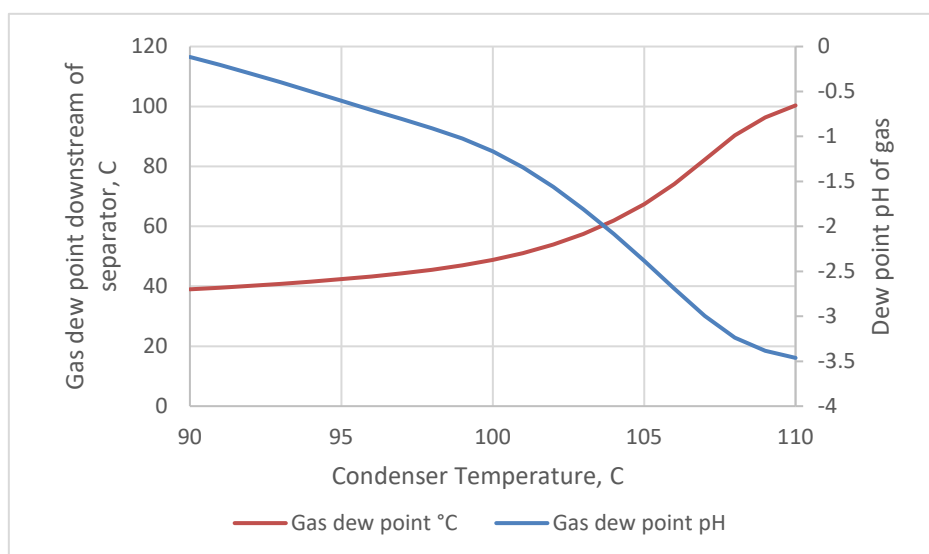

Figure 9 - dew point temperature of the gas downstream of the separator vs. the condenser temperature. the pH of the dew point liquid that is produced. The separated gas remains highly acidic

Counter-Current Decantation Process

Process Operations

Inert solids are removed from the leachate by a series of counter current decanters (CCDs). Fresh water is used and the inerts are sent to a tailings facility.

Simulation

This process is a basic washing step. Two key areas of study included the solid phases that are removed and the properties of the output liquid that is sent to the purification unit.

Figure 10 is a plot of the REE recovery efficiency and pH and in each washing unit. Recovery is computed to approach 99.3% when using four stages, 99.7% with five stages, and 99.9% with six stages. The washing efficiency in each stage is ideal since simulation software cannot predict such mechanism.
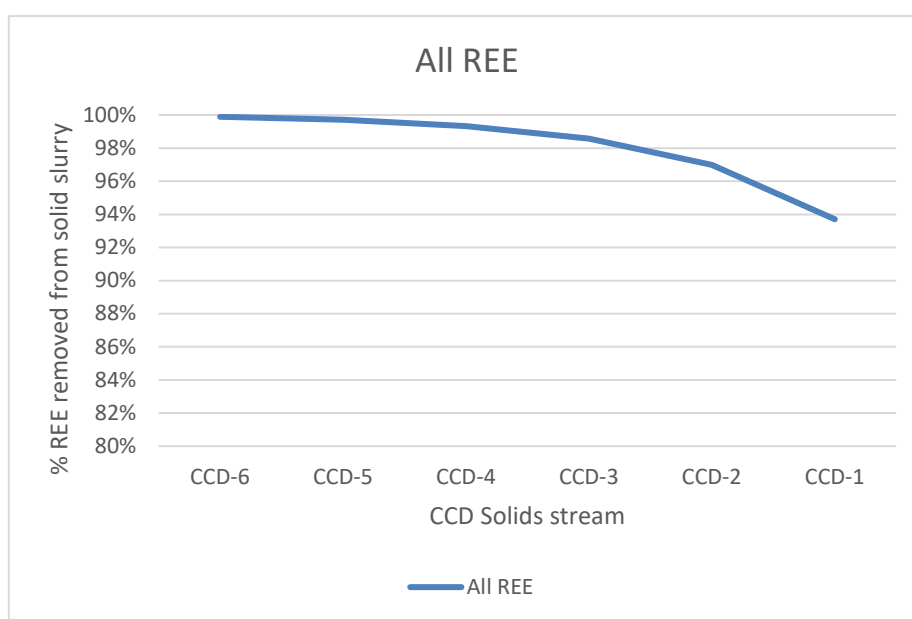

Figure 10 - Plot of fraction REE remove in each counter current washing unit

Table 7 contains the composition of the washed solids. Nearly all the material is SiO_2 and $FePO_4.2H_2O$. Other, relatively pH-independent sulfates and oxides are also computed to form.

Table 7 - Composition of key solids in the washed solids. The $GdPO_4.2H_2O$, $EuPO_4$, $NdPO_4$, and $TbPO_4$, and YPO_4 phases are purposely removed from the calcualtion because of uncertainty in predictions or precipitation kinetics. Also shown is the effect of adding $FeSO_4$ to the CCD process instead of the purification unit

	Simulated Washed solids	Simulated: when $FeSO_4$ is to the feed upstream of the CCD
SiO2	81.3%	60.6%
TiO2	0.306%	0.227%
ZrO2	0.001%	0.008%
ThO2	4e-6%	0%
FePO4.2H2O	18.3%	39.1%
BaSO₄+SrSO₄	0.001%	0.06%

The $FePO_4.2H_2O$ phase is also the phase created in the purification step when $Fe_2(SO_4)_3$ is added. It may therefore be possible to add the $Fe_2(SO_4)_3$ to the CCD unit. The far right column of Table 7 contains an updated solids flow when the $Fe_3(SO_4)_3$ additive is mixed with the quenched REE liquor (Stream 665) upstream of the CCD. This causes higher amounts of $FePO_4.2H_2O$ to precipitate in this unit. It also lowers the precipitation potential of RE-PO4 in the CCD since Fe competes with REE for the PO4 ion . Lastly, adding $Fe_2(SO_4)_3.2H_2O$ at this step lower the CCD pH slightly.

Purification Process

Process Operations

The purification unit consists of a series of stirred tanks where ferric sulfate, lime, and magnesia are added sequentially. The precipitation sequence is iron phosphates, gypsum, and aluminum and thorium hydroxide/oxide. These solids are removed by filtration. The pH is then increased further to precipitate the remaining aluminum, but since this can result in some REE losses, the solids are recycled in the purification circuit to stabilize the pH and recover the REE. Uranium is removed by IX as the final purification step.

Simulation

$Fe_2(SO_4)_3$ addition

$Fe_2(SO_4)_3$ is the first of six controlled inflows to the purification process. It removes phosphate from solution, so that RE-phosphates do not form when the pH is raised. We used a stoichiometric ratio of 1.3:1 Fe:PO_4 to set the $Fe_2(SO_4)_3$ inflow rate.

Only 38% of P(V) is removed upstream of the CaO mixer. This is because the $Fe_2(SO_4)_3$ mixer pH is 0.6, and at this pH P(V) exists primarily as H_3PO_4 with negligible amounts of PO_4^{-3}. Adding lime increases the proportion of PO_4^{-3} by ~10x, which increases the fraction of P(V) removed to 97%. The fraction of Fe^{+3} that precipitates is 89%, and the lower value reflects the excess moles of Fe(III) added relative to P(V). This indicates that optimization of $Fe_2(SO_4)_3$ and CaO addition is possible for this unit of the plant.

Table 8 - Phosphate removal following the Fe2(SO4)3 and Ca(OH)2 treatments

Stream	units	$Fe_2(SO_4)_3$ mixer	CaO mixer
Mixer pH	pH	0.6	1.8
Dissolved P(V) in inlet	% as a fx of P(V)	100%	62%
Dissolved Fe^{+3} in Inlet	% as a fx of P(V)	6%	74%
Fe(III) added	% as a fx of P(V)	106%	0%
OH-1 added	% as a fx of P(V)	0%	616%
PO4 removed as FePO4.2H2O	% as a fx of P(V)	38%	59%
PO4 remaining in solution	% as a fx of P(V)	62%	3%
Fe+3 removed as FePO4	% as a fx of P(V)	38%	61%
Fe+3 remaining in solution	% as a fx of P(V)	74%	13%
% PO4 removed	%	38%	97%
% Fe removed	%	34%	89%
% of dissolved P(V) that is H_3PO_4 at mixer pH	%	96%	66%

pH-adjustment steps

The pH adjustment process is divided into four pH-increasing steps by adding CaO , Mg(OH)$_2$, MgO(#1) and then MgO(#2). Table10 contains the reported and calculated mass of base used in the process. There is significant difference between the reported and measured values. The expectation is that the reaction of lime to raise the pH is incomplete (rate limited) and therefore, more Mg(OH)$_2$ is required to raise the pH than expected. The overall acid-base mass balance should be the same, provided that the measured and computed amounts of metal hydroxide are the same (Table 10).

Table 9 - The calculated mass rate of additives used at each process point in the Purification section. The second column is the additive purity, the third is the computed mass required, and the last is the mass required if Fe$_2$(SO$_4$)$_3$ is added in the CCD step instead (optional scenario).

Stream	Additive used at this location	Computed mass of active chemical, kg/hr	Computed mass of active chemical if Fe$_2$(SO$_4$)$_3$ is added to the CCD circuit, kg/hr
910 (Fe$_2$(SO$_4$)$_3$ reaction tank)	45% Fe$_2$(SO$_4$)$_3$	263	---
915 (Ca(OH)$_2$ reaction tank)	18% Ca(OH)$_2$	303	377
920 (MgOH$_2$ reaction tank)	20% Mg(OH)$_2$	0.2	0.2
955 (MgO #1 addition)	20% MgO	102	104
1155 (MgO#2 polisher)	20% MgO	2.5	2.4
1120 (Na$_2$CO$_3$ precipitation tank)	20% Na$_2$CO$_3$	235	238

The mass of lime predicted to raise the pH to the target is greater than the reported plant values. The cause of this difference is to be investigated. The simulation also computed that GdPO$_4$.2H$_2$O and TbPO$_4$.2H$_2$O will precipitate, but this is not observed in the plant. This discrepancy would be explained by either applying rate limiting kinetics or the need for additional solubility research.

The mass of Mg(OH)$_2$ required to raise the pH also differs from the reported measurements. The amount simulated, is the minimum value added and at that rate, the computed pH is above the target value. We think this is due to the buffering capacity of the solids being recycled. The two-step, mass addition of MgO to raise the pH is similar to the mass reported in the plant.

Table 11 contains the list of solid phases formed at each point in the process. Removing these non-valuable elements is important to create a higher purity RE$_2$(CO$_3$)$_3$ product phase.

Table 10 - List of solid phases forming at each stage of the purification process. Thirteen rare earth carbonates precipitate in the Na$_2$CO$_3$ stage (not shown in table). Cells marked in red (solid color) are the phase(s) that comprised 90+% of the solids in that stream. Those marked in diagonal hash are present in lower quantities.

Additive used	Fe$_2$(SO$_4$)$_3$	Ca(OH)$_2$	Mg(OH)$_2$	MgO_1	MgO_2	Na$_2$CO$_3$
Stream # measured	**910**	**915**	**920**	**955**	**1155**	**1150**
Al(OH)$_3$			red	red	red	hash
BaSO$_4$	hash	hash	hash			
Cd$_3$(PO$_4$)$_2$						hash
CaSO$_4$		red	red	hash		
Cu$_2$(OH)$_2$CO$_3$						hash
Fe(OH)$_3$		hash	red	hash		
FePO$_4$.2H$_2$O	red	red	red			
GdPO$_4$.2H$_2$O						hash
Mg$_3$(PO$_4$)$_2$.8H$_2$O			hash			
Mn(OH)$_2$		hash	hash	hash	hash	
SiO$_2$	hash	hash	hash	hash		
SnO$_2$	hash	hash	hash	hash		
SrSO$_4$	hash	hash	hash	hash		
TbPO$_4$.2H$_2$O			hash	hash		
ThO$_2$			hash	hash		
UO$_2$CO$_3$			hash	hash		
ZrO$_2$		hash	hash	hash		
RE$_2$(CO$_3$)$_3$						red

Table 12 contains the simulated sludge solids that exit the purification process. Gypsum precipitation at the target pH for lime addition (pH=1.8) is incomplete because much of the sulfate added is in the HSO$_4^{-1}$ form. This remaining Ca^{+2} and HSO$_4^{-1}$ eventually precipitates as gypsum at the Mg(OH)$_2$ addition step, as HSO$_4^{-1}$ is converted to SO$_4^{-2}$.

Table 11 - The waste solids that during purification and that exits the process.

	Simulated
Al(OH)3	3.6%
CaSO4.2H2O	73%
Fe(OH)3	4%
FePO4.2H2O	18%
MnO2	.1%
SiO2	.2%
TbPO4.4H2O	.4%
ThO2	.03%

Table 13 is the fraction of each element removed during the purification process. Elements that are removed completely or nearly completely, include Al, Ba, Zr, Fe, Mn, Sn, Th, and U. $TbPO_4.2H_2O$ is computed to precipitate and not be recovered with the other REE. It is possible that the thermodynamics for this phase is also uncertain and that it is recovered. Yet, there is sufficient literature data to support the predictions that it will precipitate. Several transition metals are not removed and precipitate with the $RE_2(CO_3)_3$. This is shown in Table 14.

Table 12 - The removal fraction of each element from the inlet to the purification process to the inlet of the carbonation section

Element	% removed	Element	% removed	Element	% removed
S(+6)	33%	Ti(+4)	0%	Mn(+4)	100%
P(+5)	86%	Zr(+4)	97%	Pb(+2)	0%
Al(+3)	100%	Fe(+3)	100%	Sn(+4)	99%
Si(+4)	78%	Co(+2)	0%	Th(+4)	100%
K(+1)	0%	Ni(+2)	0%	U(+6)	100%
Sr(+2)	5%	Cu(+2)	0%	Tb(+3)	100
Ba(+2)	99%	Zn(+2)	0%	Other REE	0%
		Cr(+3)	0%		

The carbonation reactions are, at this point in time, estimates. A complete thermodynamic database does not exist for RE-carbonates, and so the carbonation reactions are not modeled rigorously. Estimates for the RE-carbonates solubilities are based on the solubility of $Nd_2(CO_3)_3$, which is available. In upcoming work, a RE-carbonate database will replace the values presented here. The differences are expected to be nominal, since the solubility of these carbonates are relatively low. Thus, the absolute mass of solids recovered should not change, but the concentration in the remaining liquor will.

Table 13 - The solid phases forming in the soda ash treatment section. The left column contains the Rare earth phases. The right column contains the acid-soluble impurities.

Rare earth carbonates	Rare earth carbonates	Impurities
$Y_2(CO_3)_3$	$Ho_2(CO_3)_3$	$Al(OH)_3$
$Dy_2(CO_3)_3$	$La_2(CO_3)_3$	$Ca_3(PO_4)_2$
$Er_2(CO_3)_3$	$Tm_2(CO_3)_3$	$Cu_2(OH)_2CO_3$
$Yb_2(CO_3)_3$	$Lu_2(CO_3)_3$	$Fe(OH)_3$
$Ce_2(CO_3)_3$	$Pr_2(CO_3)_3$	$Mg_3(PO4)_2.8H_2O$
$Nd_2(CO_3)_3$	$Eu_2(CO_3)_3$	MnO_2
$Sm_2(CO_3)_3$	$GdPO_4.2H_2O$	$SrSO_4$
		ZrO_2

DISCUSSION/CONCLUSIONS

Process Operations

The simulation has shown that some aspects of the process can be modelled using the thermodynamic model but that there are still some significant limitations in the models that do not allow accurate estimation of the components that will precipitate in the process flow sheet.

Simulation

The purpose of the simulation study was to determine if it were beneficial to use rigorous thermodynamics to model and optimize a REE purification plant. We conclude the following challenges and accomplishments from this work.

1. Challenge – There are rate-limiting precipitation and dissolution processes that cannot be simulated with equilibrium models. Empirical inefficiencies would be needed to match some plant observations. This will hopefully compensate for the differences in the lime and MgO requirements predicted vs. measured.

2. Challenge – The breadth of RE chemistry is broad and ranges with temperature (25 to 275 C) and counterion (PO_4^{-3}, SO_4^{-2}, OH^{-1}, $CO3^{-2}$, O^{-2}). A partially complete database achieves a partial solution as expected. The completed database, containing the phosphate and carbonate phases will provide better studies. This will eliminate predictions like YPO4 precipitating in the kiln wash and CCD solids.

3. Accomplishments – the ionic liquid activity model was robust enough to handle the VLE of the kiln outlet.

4. Accomplishments – the database is sufficiently completed to predict the phase behavior of the nineteen non-RE metals in the digested ore.

5. Accomplishment – the simulation approach allowed us to look at the implications for changing the processing, such as adjusting the gas cooling temperature to manage condensate corrosion or to adjust the $Fe_2(SO_4)_3$ treatment location so that the potential for RE to precipitate is lowered.

REFERENCES

1. Anderko, D. A. (2020, Jan 7). CTO, OLI Systems, Inc. (A. Gerbino, Interviewer)

2. Das, G., Lencka, M., Eslamimanesh, A., Anderko, A., & RIman, R. (2017). Rare-earth elements in aqueous chloride systems: Thermodynamic modeling of binary and multicomponent systems in wide concentration ranges. *Fluid Phase Equilibria*, 16-57.

3. Wang, P., & Anderko, A. (2011). Modeling chemical equilibria, phase behavior, and transport properties in ionic liquid systems. *Fluid Phase Equilibria*, 74-82.

4. Gausse, C.,Szenknect, S., Qin, D. W., Mesbah, A., Clavier, N.,Neumeier, S.; Bosbach, D.; Dacheux, N., Determination of the solubility of rhabdophanes LnPO4. 0.667 H_2O (Ln= La to Dy). *Eur. J. Inorg. Chem.* **2016,** *28*, 4615-4630

5. Firsching, F. H.; Brune, S. N., Solubility products of the trivalent rare-earth phosphates. *J. Chem. Eng. Data* **1991,** *36* (1), 93-95

6. Liu, X.; Byrne, R. H., Rare earth and yttrium phosphate solubilities in aqueous solution. *Geochim. Cosmochim. Acta* **1997,** *61* (8), 1625-1633